

# Multi-performance Target Collaborative Optimization Methods for Battery Electric Vehicle

Chen Yawei

Chongqing Jiaotong University

Chen Qian

Chongqing Jiaotong University

Liu Jurui

ji lin jian zhu gong cheng xue yuan: Jilin Jianzhu University

Hao Xixiang

Chongqing Jiaotong University

Yuan Chenheng (✉ [yuanchenheng@163.com](mailto:yuanchenheng@163.com))

Chongqing Jiaotong University <https://orcid.org/0000-0003-4376-8194>

---

## Original Article

**Keywords:** Battery Electric Vehicle (BEV), Multi-objective Optimization, Pareto Optimum Principle, 19 Evolutionary Algorithm

**Posted Date:** September 20th, 2021

**DOI:** <https://doi.org/10.21203/rs.3.rs-895705/v1>

**License:**  This work is licensed under a Creative Commons Attribution 4.0 International License.

[Read Full License](#)

---

1                   Multi-performance Target Collaborative Optimization Methods for  
2                   Battery Electric Vehicle

3                   Yawei Chen<sup>1</sup>, Qian Cheng<sup>1</sup>, Jurui Liu<sup>2</sup>, Xixiang Hao<sup>3</sup> Chenheng Yuan<sup>4,\*</sup>

4                   **Abstract:** The present studies on battery electric vehicles (BEVs) has mainly focused on the single-objective  
5                   or weighted multi-objective optimization based on energy management, which can not manifest the coupling  
6                   relationship among the vehicle performance objectives essentially. To optimize the handling stability, ride comfort  
7                   and economy of BEV, this paper built the stability dynamics analysis model, ride comfort simulation half-car  
8                   model and power consumption calculation model of BEV, as well as two-point virtual random excitation model on  
9                   Level B road and proposed related evaluation indexes, including vehicle handling stability factor, weighted  
10                  acceleration root-mean-square (RMS) value of vertical vibration at the driver's seat and power consumption per  
11                  100 m at a constant speed. The Pareto optimum principle-based multi-objective evolutionary algorithm (MOEA)  
12                  of BEV was also designed, which was encoded with real numbers and obtained the target values of all optional  
13                  schemes via MATLAB/Simulink simulation software. The merits and demerits of alternative schemes could be  
14                  judged according to the Pareto dominance principle, so that alternative schemes obtained after optimization were  
15                  realizable. The results of simulation experiment suggest that the proposed algorithm can perform the  
16                  multi-objective optimization on BEV, and obtain a group of Pareto optimum solutions featured by high handling  
17                  stability, favorable ride comfort and low energy consumption for the decision-makers.

18                   **Keywords:** Battery Electric Vehicle (BEV); Multi-objective Optimization; Pareto Optimum Principle;  
19                   Evolutionary Algorithm

20  
21                  <sup>1</sup>

---

<sup>1</sup> \*Corresponding author E-mail: yuanchenheng@163.com (C. Yuan)

<sup>4</sup>Chongqing Jiaotong University College of Traffic & Transportation, Chongqing 400074, China.  
Full list of author information is available at the end of the article

22    **0 Introduction**

23       The efficient operation of BEV entails the coordination of handling stability, ride comfort and economy, with  
24       non-differentiable, discontinuous, hybrid, multidimensional, constrained and nonlinear characteristics in its model,  
25       which is a typical hybrid nonlinear multi-objective optimization issue. Els et al. optimized the suspension  
26       characteristic parameters with dynamic-Q algorithm, for the multi-objective optimization of vehicle handling  
27       stability and ride comfort, and provided a set of suspension parameters which can improve vehicle handling  
28       stability and ride comfort for decision makers<sup>[1]</sup>. Yang Guangci et al. optimized the fuel consumption, HC+NOx  
29       emissions and CO emissions of hybrid electric vehicle (HEV), and proposed a multi-objective optimization  
30       evolutionary algorithm based on the Pareto optimum principle for HEV, thus obtaining the Pareto optimum  
31       solution set with low fuel consumption and low emissions<sup>[2]</sup>. Zhang Jingmei et al. improved the genetic algorithm  
32       to realize the multi-objective comprehensive optimization of ride comfort, handling stability and road-friendliness  
33       of vehicles, and obtained the best matching value of suspension stiffness and damping<sup>[3]</sup>. Yang Rongshan et al.  
34       balanced and optimized handling stability and ride comfort of vehicles with approximate model, and then obtained  
35       the optimum value of suspension stiffness, damping and stabilizer bar<sup>[4]</sup>. Ding Xiaolin et al. proposed a  
36       multi-objective optimization matching method for driving system parameters, to improve the ride comfort of  
37       four-hub motor-driven electric vehicles and reduce the energy consumption<sup>[5]</sup>. Song Kang et al. conducted the  
38       optimized analysis on suspension and seat parameters based on ride comfort of vehicles, and built a  
39       multi-objective optimization model of vehicle dynamic performance. Non-dominated sorting genetic algorithm  
40       (NSGA-II) with elite strategy was selected to solve the optimization model, and the Pareto optimum solution set  
41       and Pareto frontier were obtained<sup>[6]</sup>. Chen Yikai et al. determined the optimum control parameters to make road  
42       friendliness and ride comfort of vehicles comprehensively through range and variance analysis, in order to  
43       improve road friendliness and ride comfort of vehicles at the same time. The simulation results show that the

44 multi-objective optimum control strategy can make the vehicle comfortable and robust to the change of pavement  
45 grade<sup>[7]</sup>. Zhang Zhifei et al. took the vertical acceleration of the driver and the frame and the sum of the 95th  
46 percentile to the fourth power as the performance optimization indexes, to normalize the weight of indexes to a  
47 single-objective function by analytic hierarchy process for improving ride comfort and road friendliness of  
48 commercial vehicles, as well as optimizing the stiffness and damping of suspension by genetic algorithm. The  
49 simulation results show that ride comfort and road friendliness of optimized vehicles are improved effectively<sup>[8]</sup>.  
50 Yang Kun et al. conducted parameter sensitivity analysis on ride comfort and road friendliness of six-axle  
51 semitrailer with the optimal Latin hypercube experimental design method, selected appropriate parameters  
52 combined with the actual situation and optimized ride comfort, road friendliness, the comprehensive performance  
53 of ride comfort and road friendliness with neighborhood cultivated multi-objective genetic optimization  
54 algorithm. The research results show that under the common driving speed, the evaluation indexes of selected  
55 optimization scheme, smoothness and road friendliness can also be better optimized<sup>[9]</sup>. Zhou Feikun et al. carried  
56 out multi-objective optimization on parameter matching of dynamical system with the optimization method of  
57 SAPSO with average mileage under multiple working conditions, average total energy consumption under  
58 multiple working conditions and complete vehicle kerb mass as the specific targets. The simulation results show  
59 that the weight of vehicles can be reduced and the economic performance on the premise of ensuring the dynamic  
60 performance can be improved<sup>[10]</sup>. Zhang Kangkang et al. compared and selected the 3 dynamical system  
61 matching projects with maximum speed, acceleration time and power consumption per 100 km as the specific  
62 targets, solved the problem of conflicting among indexes to be optimized with the multi-objective genetic  
63 algorithm, described the competitive relationship between indexes with the Pareto matrix, and clearly defined the  
64 constraints and scope of application of policies<sup>[11]</sup>.

65 Most of the above studies transformed the multi-objective optimization to single-objective optimization  
66 through weighting or other methods, and then obtained the solution through mathematical programming.

67 Therefore, they have the following weaknesses: (1) The decision-makers were needed to provide profound  
68 preference knowledge (i.e. weight coefficient of each target), to build single-objective evaluation function; (2) A  
69 majority of single-objective optimization technologies were based on local optimization search algorithm. Despite  
70 the local or global optimum solution obtained for single-objective optimization, several optimum solutions that  
71 are available couldn't be searched concurrently, thus, the flexible requirements of multi-objective decision can be  
72 hardly met.

73 In addition, most of the optimization objectives in the researches on single-objective or multi-objective  
74 optimization were vehicle handling stability or ride comfort but the researches about the multi-performance target  
75 collaborative optimization of handling stability, ride comfort and economy of BEVs could be seldom found. For  
76 this reason, this paper built the stability dynamics analysis model, the ride comfort simulation half-car model and  
77 the power consumption calculation model, as well as the two-point virtual random excitation model of Level B  
78 road surface, respectively, with BEV as the research object, and proposed the evaluation indexes corresponding to  
79 the multi-performance objectives by highlighting the multi-objective optimization of BEVs' handling stability,  
80 ride comfort and economy under the turning condition, with simulation verification on handling stability, ride  
81 comfort and economy of BEVs based on Pareto optimal algorithm. The simulation results show that the proposed  
82 Pareto optimal algorithm can collaboratively optimize the safety, ride comfort and economy of BEVs, with the  
83 improvement of handling stability, ride comfort and economy to a certain extent.

84 The innovation points of this paper include: 1) Based on the improved optimization algorithm of  
85 non-dominated genetic algorithm, the elite strategy was introduced, with congestion distance and its comparison  
86 operator as the basis of secondary sorting. Finally, the global optimal Pareto optimum solution and Pareto front  
87 edge were obtained. 2) With handling stability, ride comfort and economy of BEVs as optimization objectives for  
88 the first time, the key parameters related to multiple performance were selected as design parameters, to realize  
89 the multi-objective optimization of dynamical performance of BEVs, and the optimal matching scheme of several

90 key parameters was obtained. 3) The optimization ideas and methods have important theoretical significance and  
91 engineering practical application value for the optimization design of multi-objective parameters including other  
92 mechanical properties of BEVs, such as handling stability transient response analysis and transmission  
93 performance.

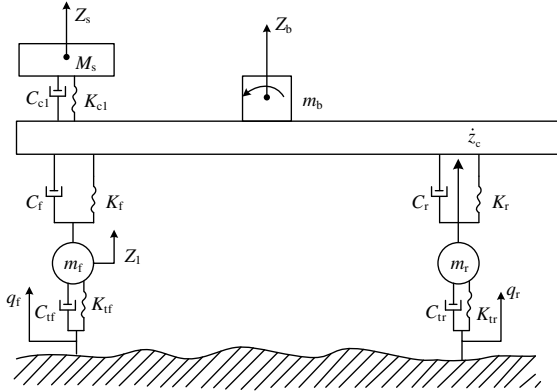
94 **1 Vehicle Dynamics Models**

95 **1.1 Vehicle Dynamics Half-car Model**

96 Vehicles receive inputs from longitudinal, vertical, and transverse directions, from which, the motion  
97 response characteristics are definitely interactive and coupled mutually. The influence of vertical coupling motion  
98 generated by the listing under the working condition of uniform turning movement on the vertical comfort of the  
99 driver can be ignored. Therefore, this paper considered the vertical motion of vehicles alone when building ride  
100 comfort model. First of all, the complex vehicle system was properly simplified and assumed:

101 1) Vehicles are symmetrical to the longitudinal symmetry plane and road unevenness corresponding to the  
102 four tires is the same; 2) It is assumed that the road unevenness conforms to the normal distribution of each state  
103 after a stationary random process, the road unevenness corresponding to each tire on the same side is different,  
104 with a response time delay caused by the wheelbase; 3) Both the stiffness of tires and seats are simplified into  
105 linear function; Suspension damping is a linear function of speed; 4) Each tire has a single contact with the  
106 ground , without any bounce; Road excitation acts on the central point of contact between tires and the road  
107 surface..

108 After linearizing the automobile system into a half simplified model approximately, front and rear tires will  
109 bear 2 random inputs, and the free-body diagram is shown as Figure 1.  
110



111

112

Figure 1 Vehicle 4-DOF Model

113 All parameters in Figure 1 are set as follows:  $m_b$  is curb weight;  $I_b$  is vehicle turning inertia;  $m_f$  and  $m_r$   
 114 are unsprung mass of front suspension and rear suspension, respectively;  $K_{c1}$  and  $C_{c1}$  are spring stiffness and  
 115 damping of driver seat, respectively;  $K_f$  and  $C_f$  are spring stiffness and damping of front suspension,  
 116 respectively;  $K_r$  and  $C_r$  are spring stiffness and damping of rear suspension, respectively;  $K_{tf}$  and  $C_{tf}$  are  
 117 stiffness and damping of front tires, respectively;  $K_{tr}$  and  $C_{tr}$  are stiffness and damping of rear tires, respectively;  
 118  $q_f$  and  $q_r$  are vertical displacement excitation of front and rear tires, respectively.

119 According to D'Alembert's principle, the differential equation of vibration motion of 4-DOF can be  
 120 expressed as:

$$121 \quad M\ddot{Z} + C\dot{Z} + KZ + C_q\dot{Q} + K_qQ = 0 \quad (1)$$

122 Where,  $Z = [Z_1, Z_b, Z_c, Z_s]^T$ ;  $Z_s$ ,  $Z_b$ ,  $Z_1$  and  $Z_c$  are vertical vibration displacement of driver seat, vehicle  
 123 body, front suspension and rear suspension, respectively;  $M$  is mass matrix;  $C$  is system damping matrix;  $K$  is  
 124 system stiffness matrix;  $K_q$  is road excitation stiffness; and  $Q$  is road excitation displacement. According to  
 125 Literature [12], the linear inhomogeneous equation set of 4 frequency response functions within the range of  
 126 frequency domain can be obtained from Formula (1):

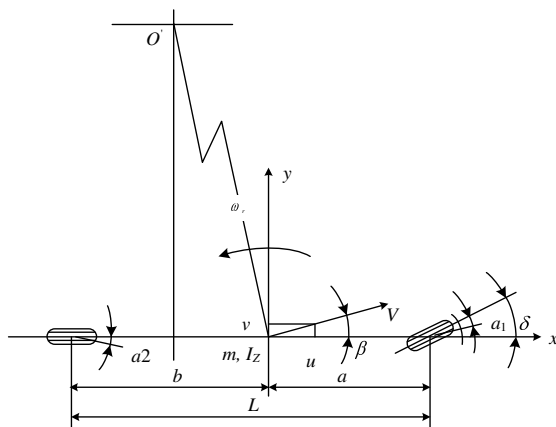
$$127 \quad A_{6 \times 6} \times [H_1 \ H_2 \ H_3 \ H_4]^T \\ = [Q_1 \ Q_2 \ Q_3 \ Q_4]^T \quad (2)$$

128  $A_{6 \times 6}$  is the response coefficient matrix of each response frequency. It has been verified that its rank is

129 related to its augmented matrix  $B_{4 \times 5}$ , so the equation set has a solution. In the formula,  $[H_1 \ H_2 \ H_3 \ H_4]$   
 130 correspond to 4 vibration responses relative to the frequency response function vector of the front tire random  
 131 excitation input  $[H_{\tilde{z}1-\tilde{q}_f}, H_{\tilde{z}b-\tilde{q}_f}, H_{\tilde{z}c-\tilde{q}_f} \text{ and } H_{\tilde{z}s-\tilde{q}_f}]^T$ , and the frequency response function of seat acceleration  
 132 can be finally obtained.

## 133 1.2 Handling Stability Model

134 Handling stability of vehicles when driving mainly includes longitudinal stability and lateral stability.  
 135 Longitudinal stability may be out of control mainly in course of longitudinal driving on slope. Lateral stability is  
 136 mainly reflected in the form of cross slip or rollover. Listing motion is produced when vehicle makes a turn at a  
 137 uniform speed and the vehicle inclination leads to lateral deformation of the suspension system. The complete  
 138 vehicle model simplified into a 2-DOF system with lateral oscillation rotating z axis and lateral motion rotating y  
 139 axis alone is shown in Figure 2 <sup>[13]</sup>. Then, vehicle listing dynamics model was established, i.e., the relation  
 140 between the listing stability factor, the listing characteristics of suspension and the dynamic load generated by the  
 141 road random excitation.



142  
143 Figure 2 Vehicle Model of 2-DOF

144 In Figure 2,  $\alpha_1$  and  $\alpha_2$  are slip angle of front and rear tires;  $\beta$  is slip angle of vehicle centroid;  $\delta$  is front  
 145 wheel angle;  $\omega_r$  is speed of heading angle;  $m$  is total weight of vehicles;  $I_z$  is rotational inertia of vehicle  
 146 rotating z axis;  $a$  and  $b$  are the distance from front axis and rear axis to vehicle centroid, respectively;  $u$  and  $v$

147 are weight of speed  $V$  of vehicle centroid on  $x$  axis and  $y$  axis.

148 Supposed that vehicle vertical displacement and lateral displacement are all zero, the systematic differential  
149 equation of motion can be expressed as below by ignoring the influence of suspension temporarily under the input  
150 of front wheel, and considering the planar motion of vehicle alone.

151 
$$(k_1 + k_2)\beta + \frac{1}{u}(ak_1 - bk_2)\omega_r - k_1\delta = m(\dot{v} + u\omega_r) \quad (3)$$

152 
$$(ak_1 - bk_2)\beta + \frac{1}{u}(a^2k_1 + b^2k_2)\omega_r - ak_1\delta = I_z\dot{\omega}_r \quad (4)$$

153 When the vehicle is moving at a constant circular motion type,  $\dot{\omega}_r = 0$  and  $\dot{u} = 0$ , and the vehicle steering  
154 sensitivity,  $\gamma = \omega_r/\delta$ , can be obtained.  $k_1$  and  $k_2$  are the cornering stiffness of front and rear tires, respectively.

155 According to Formula (3) and Formula (4), stability factor can be expressed as:

156 
$$K = \frac{m}{L^2} \left( \frac{a}{k_2} - \frac{b}{k_1} \right) \quad (5)$$

157 The tire cornering stiffness is closely related to the tire vertical load, which can be expressed as:

158 
$$k_{il(r)} = 0.06778F'_{zil(r)}^2 - 9.144F'_{zil(r)} + 5.129 \quad (6)$$

159 Where,  $F'_{zil(r)}$  is the tire load of front and rear axles, respectively.  $l$  and  $r$  mean the left side and the right  
160 side.

161 
$$F'_{zil(r)} = F_{zil(r)} + \Delta F_{zil(r)} + F_{id} \quad i = 1, 2 \quad (7)$$

162 Where,  $F_{zil(r)}$  is the vertical reaction force of ground of front and rear axles and left (right) tire under an  
163 idle status. The amount of change of vertical load includes two parts:  $F_{id}$ , i.e., the dynamic load applied to front  
164 and rear axles respectively by road random excitation and  $\Delta F_{zil(r)}$ , the amount of change of vertical reaction  
165 applied to front and rear axles and left (right) tire by the centrifugal force. Therefore, the improved stability factor  
166 can be expressed as:

167 
$$K_{l(r)} = \frac{m}{L^2} \left( \frac{a}{k_{2l(r)}} - \frac{b}{k_{1l(r)}} \right) \quad (8)$$

168 2 Two-point Virtual Random Excitation Model of Road Surface

The road excitation born by vehicles in driving belongs to multiple-support excitation. In consideration of the large wheel base, front and rear tires have receive stable and hysteresis road excitation of different phrases. A road model is built within the frequency domain by taking Level B road surface as an example<sup>[14]</sup>. Suppose that front and rear tires receive the same related stable road excitation, the two excitation points of road surface can be expressed as:

$$174 \quad \left\{ Q_{(t)} \right\} = \begin{bmatrix} Q_1 \\ Q_2 \end{bmatrix} = \begin{bmatrix} Q(t-t_1) \\ Q(t-t_2) \end{bmatrix} \quad (9)$$

175        $Q_{(t)}$  can be regarded as the generalized single point excitation. Suppose that the auto-spectral density of  $Q_{(t)}$   
 176      is a known constant, and the exciting moment born by front and rear tires is  $t_1$  and  $t_2$ , respectively, the  
 177      two-point virtual excitation model obtained with pseudo excitation method can be expressed as:

$$178 \quad [\tilde{q}(\omega)] = \sqrt{S_{qq}(\omega)} \begin{bmatrix} e^{-j\omega t_1} \\ e^{-j\omega t_2} \end{bmatrix} e^{j\omega t} = \begin{bmatrix} \tilde{q}_f \\ \tilde{q}_r \end{bmatrix} \quad (10)$$

179 Where,  $\tilde{q}_f$  and  $\tilde{q}_r$  are virtual excitations born by front and rear tires, respectively.

180 3 Vehicle Multi-performance Evaluation Indexes

### 181 3.1 Evaluation Index of Handling Stability

Handling stability of vehicles covers a broad range, which is mainly manifested by the time-frequency response characteristics of vehicles in curve driving. When a vehicle turns a corner at a constant speed, the ratio of yaw velocity to the turning angle of front wheel at a stable state is used as the response evaluation standard. Differently, the value of stable state factor manifests the stable response of vehicles. Generally speaking, the influence of vehicle structure parameters is considered only in the research analysis of stable state response of vehicle when turning a corner. Hence, the influence of dynamic load caused by road random excitation and suspension stiffness and damping and obtaining the improved stability factor was introduced in this paper, so that

189 the research of vehicle stability can be more accurate. The improved stability factor  $K_{l(r)}$  in Formula (8) was  
190 taken as the evaluation index of listing handling stability here in this paper.

191 **3.2 Evaluation Index of Ride Comfort**

192 According to GB/T 4970-2009 *Test Method of Vehicle Ride Comfort*, this paper analyzed the vertical  
193 acceleration of the driver's seat instead of human body acceleration with the weighted acceleration RMS value  
194 corresponding to the human body acceleration transferred through seat as the evaluation index of ride comfort.  
195 Taking the weighted acceleration RMS value  $\sigma_{\ddot{z}_S}$  of the vertical vibration at driver's seat as the evaluation index  
196 of ride comfort, then the formula can be expressed as:

$$197 \quad \sigma_{\ddot{z}_S} = \sqrt{\int_0^{\infty} W_{zs}^2(\omega) |H_{\ddot{z}_S-\ddot{q}_f}|^2 G_{\ddot{z}_{qf}}(f) df} \quad (11)$$

198 Where,  $W_{zs}(\omega)$  is weighting function (the value is 1 here);  $G_{\ddot{z}_{qf}}(\omega)$  is power spectral density inputted by  
199 front axle road excitation;  $H_{\ddot{z}_S-\ddot{q}_f}$  is vertical acceleration frequency response function of driver's seat.

200 **3.3 Evaluation Index of Economy**

201 As the research object, the economy of BEVs is generally evaluated by its power consumption per 100 km at  
202 a constant speed. Under the uniform driving condition, the driving force required by the vehicle  $F$  includes  
203 listing resistance  $F_f$  and air resistance  $F_w$ , i.e.,  $F = F_f + F_w$ . The power consumption per 100 km of vehicle  
204 driving at a constant speed can be calculated with the following formula:

$$205 \quad E_{drive} = \frac{(F_f + F_w)S}{\eta_{mc} \cdot \eta_T \cdot \eta_q} = \frac{\left( mgf + \frac{C_D A u_a^2}{21.15} \right) S}{\eta_{mc} \cdot \eta_T \cdot \eta_q} = \frac{mgf + \frac{C_D A u_a^2}{21.15}}{36(\eta_{mc} \cdot \eta_T \cdot \eta_q)} \quad (12)$$

206 Where,  $S = 100km$ ,  $f$  is listing resistance coefficient,  $C_D$  is air resistance coefficient,  $A$  is windward  
207 area,  $u_a$  is vehicle driving speed,  $\eta_{mc}$  is the efficiency of motor and controller,  $\eta_T$  is the total efficiency of  
208 drive system and  $\eta_q$  is the average discharging efficiency of accumulator.

209

210 **4 Mathematical Modeling of Multi-objective Optimization**

211 **4.1 Mathematical Description of Multi-objective Optimization**

212 BEV optimization in this paper means optimizing the parameters of suspension system and battery control  
213 strategy on the basis of satisfying all constraints, so as to make the vehicle safe, comfortable and energy-saving  
214 under certain conditions and make several target functions in conflict realize the optimal status within a feasible  
215 region. Suppose that  $X$  is the decision space of  $n$ -dimension and  $Y$  is the target space of  $n$ -dimension on the  
216 basis of ensuring the loss of generality, then its mathematical modeling of multi-objective optimization can be  
217 expressed as<sup>[11]</sup>:

$$\begin{aligned} \min y &= F(x) = [f_1(x) f_2(x) \cdots f_m(x)] \\ \text{s.t. } g_i(x) &\leq 0 \quad (i=1,2,\dots,q_1) \\ h_i(x) &= 0 \quad (j=1,2,\dots,q_2) \end{aligned} \tag{13}$$

219 Where,  $x = [x_1 x_2 \cdots x_n] \in X \subset R^n$  is decision vector;  $y = [y_1 y_2 \cdots y_n] \in Y \subset R^m$ . The objective function  
220  $F(x)$  means  $m$  mapping functions  $f: X \rightarrow Y$ ,  $g_i(x) \leq 0$  ( $i = 1, 2, \dots, q_1$ ) and  $h_j(x) = 0$  ( $j = 1, 2, \dots, q_2$ ) are the  
221  $q_1$  inequation constraints and  $q_2$  equation constraints that the objective function  $F(x)$  needs to satisfy.

222 **4.2 Optimization of Objectives**

223 The driving conditions set for optimization play a key role, for the speed and road conditions of the vehicle  
224 always change in driving. According to the driving conditions set in this paper, the vehicle can be driven stably at  
225 a constant speed (30 km/h) along Level B curved road with a 50 m turning radius. Generally speaking, vehicle  
226 vibration becomes the most obvious and even resonance may be produced when excitation frequency is 3.15 Hz.  
227 In other words, the vehicle's ride comfort and handling stability become the most sensitive. Therefore, the analysis  
228 on multi-performance optimization was optimized at a road excitation frequency of 3.15 Hz<sup>[12]</sup>.

229 This paper took function  $\min\sigma_{zs}$  (acceleration RMS value  $\sigma_{zs}$  of the vertical vibration at the driver's seat),  
230  $\min E_{drive}$  (power consumption per 100 km at a constant speed) and handling stability factor  $K_{l(r)} > 0$ , which mean

231 reducing the acceleration RMS value of the vertical vibration at the driver's seat and power consumption per 100  
 232 km at a constant speed and making the vehicle lack of turning characteristics properly, as the optimization  
 233 objectives to meet the requirements of handling stability and ride comfort, and minimize power consumption as  
 234 much as possible. Set the following functions:

$$235 \quad \begin{cases} f_1(x) = K_{l(r)} \\ f_2(x) = \sigma_{zs} \\ f_3(x) = E_{drive} \end{cases} \quad (14)$$

236 Where,  $x$  is decision variables (or parameters to be optimized), decision variables and corresponding  
 237 constraint conditions, all of which vary along with specific optimized objects.

### 238 4.3 Selection of Design Variables

239 The parameters which exert significant influence on the optimization objectives were optimized in this paper.  
 240 The stiffness of front and rear suspensions and damping of the vehicle are closely related to ride comfort of the  
 241 vehicle; Meanwhile, vertical load of each vehicle axle changes when the vehicle is listing under the effect of road  
 242 excitation, moment resulting from sidesway and centripetal force, which means the load that each axle bears has  
 243 been allocated again in listing, causing the change of cornering stiffness of left and right tires or inside and outside  
 244 tires, and finally changing the steady state response of the vehicle, as well as the stability factor. Therefore, the  
 245 stiffness and damping of front and rear suspensions can be regarded as variables of optimization analysis. In  
 246 consideration of the significant influence of related parameters of BEV's motor and battery on battery energy  
 247 consumption, some parameters selected also serve as design variables. All optimized parameters and their  
 248 selection range are shown in Table 1.

249 Table 1 Parameters to Be Optimized and Constraint Range

Type of Parameters	Constraint Range
Maximum power of motor/kw	$P_e \in [20, 100]$
Power coefficient of motor	$R_s \in [0.6, 1.5]$

Number of battery pack modules/piece	$N_b \in [20, 30]$
Axle ratio	$R_m \in [0.5, 2.5]$
Upper limit of battery status/%	$H_{SOC} \in [0.55, 0.8]$
lower limit of battery status/%	$L_{SOC} \in [0.2, 0.55]$
Drive limiting speed/(kw/h)	$V_e \in [5, 100]$
Front suspension stiffness/(N/m)	$K_f$ $\in [10475, 37046]$
Front suspension damping/(N · s/m)	$C_f \in [2500, 6000]$
Rear suspension stiffness/(N/m)	$K_r$ $\in [16800, 46320]$
Rear suspension damping/(N · s/m)	$C_r \in [1200, 3600]$
Suspension dynamic deflection/(mm)	$f_d \in [30, 60]$

250

251 **4.4 Pareto Optimum Principle**

252 Pareto optimum principle serves as a key concept in game theory. Several key concepts are given below

253 based on the symbol definitions in 4.1 <sup>[15]</sup>.254 Definition 1 Pareto dominance. For random vector  $u = [u_1 u_2 \cdots u_m] \in Y, v = [v_1 v_2 \cdots v_m] \in Y$ , if and only if255  $\forall i \in \{1, 2, \dots, m\}: u_i \geq v_i \wedge \exists j \in \{1, 2, \dots, m\}: u_j > v_j$  is true,  $v$  is superior to  $u$ , or  $v$  dominates  $u$ , which can be256 written as  $u \prec v$ .257 Definition 2 Pareto optimum solution.  $x \in X$  is called Pareto optimum solution (or non-dominated solution

258 and non-inferior solution), if and only if

259  $\rightarrow \exists x' \in X: F(x') = [f_1(x') f_2(x') \cdots f_m(x')] > F(x) = [f_1(x) f_2(x) \cdots f_m(x)]$ . Pareto optimum solution is not

260 dominated by other solutions with the least goal conflict, which can provide decision-makers with a better space

261 for choosing, and can help them make decisions according to the environment or requirements when it is applied

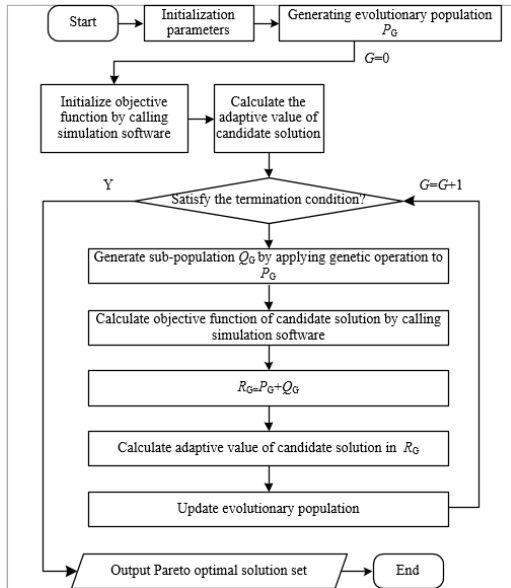
262 to engineering.

263 **5 Algorithm Design**

264       Taking the handling stability factor  $f_1(x) = K_{l(r)} > 0$ , acceleration RMS value of vertical vibration at the  
265       driver's seat  $f_2(x) = \min\sigma_{zs}$  and power consumption per 100 km at a constant speed  $f_3(x) = \min E_{drive}$ , which  
266       mean making the vehicle lack of turning characteristics properly and reducing the acceleration RMS value of the  
267       vertical vibration at driver's seat and power consumption per 100 km at a constant speed as the optimization  
268       objectives, this paper proposed the Pareto Optimum Principle-based Multi-Objective Evolutionary Algorithm of  
269       EV (EV-MOEA), which is an improvement of non-dominated genetic algorithm (NSGA), with the optimization  
270       considering each target equally important and dealing with multi-objective problems, i.e. introducing the elite  
271       strategy in the evolutionary process, with the crowding distance and its comparison operator as the basis of the  
272       secondary sorting. Finally, the global Pareto optimum solution and the Pareto frontier are obtained.

273       The advantages of EV-MOEA designed in this paper include good exploration performance, used the fast non  
274       dominated sorting, reduce the complexity of the non inferior sorting genetic algorithm, with fast non-dominant  
275       ranking, complexity of noninferior sorting genetic algorithm, replacing sharing radius with crowding distance and  
276       crowding distance comparison operator, as well as fast running speed, which improve the accuracy of the  
277       optimization results in a limited way, so that the individuals in the quasi-Pareto domain can extend to the whole  
278       Pareto domain and distribute evenly. Introducing the elite strategy maintained the diversity of the population, with  
279       good convergence of the solution set, which improved the rapidity and robustness of the optimization algorithm.

280       EV-MOEA has an evolution population, and each candidate solution is expressed by real number encoding.  
281       The main procedures of the algorithm are shown in Figure 3.



282

283

284     The algorithm is calculated as the steps below:

285         (1) Initialization. Contents in need of initialization mainly include: Scale of evaluation population  $N$ ,  
 286         crossover probability  $P_c$ , mutation probability  $P_m$ , maximum generation  $G_{max}$ , vehicle model parameters to be  
 287         optimized, vehicle driving conditions required for simulation, specific performance indexes to be optimized  
 288         required for the vehicle model, decision space  $R^m$  of  $m$  decision variables ( $X_1, X_2, \dots, X_m$ ), i.e.  $X_i$   
 289          $[L_i, H_i] (i=1, 2, \dots, m)$  (where,  $L_i$  and  $H_i$  mean lower limit and upper limit of  $X_i$ , respectively). For the engineering  
 290         application, the precision that can be realized by each parameter of BEV is limited certainly, which is significant  
 291         only when the value of decision variables is within the range of realizable precision. The significant digit of  
 292         variables in this paper is set according to precision limitation and maximum generation, with the maximum  
 293         evolutionary algebra as the condition for judging the completion of evolutionary process. Therefore, the  
 294         evolutionary algebraic counter  $G$  needs to be set and initialize into  $G = 0$ .

295         (2) Evolutionary population generation. The candidate solution is represented by real coding. The process of  
 296         generating candidate solution gene is as below: First, generate the evaluation  
 297         population  $P_G = \{x_j = (x_1 x_2 \dots x_i \dots x_m) \mid x_i \in [L_i, H_i], j = (1, 2, \dots, N), i = (1, 2, \dots, m)\}$  with uniform random  
 298         number generator, and then truncate the value exceeding the significant digit in  $x_i$  (rounded-off) according to the

299 set significant digit.

300 (3) Simulation software calling to initialize the objective function value. Let  $\forall x_j \in P_G$ , call *MATLAB/Simulink* software to test the performance of vehicle model corresponding to  $x_j$ . Simulate the status of the vehicle when driving under specified road conditions and obtain function values of each objective according to the returned results if the performance constraint conditions can be met. To be specific,  $f_1(x_j)$  is stability factor,  $f_2(x_j)$  is the acceleration RMS value of vertical vibration at driver's seat and  $f_3(x_j)$  is the power consumption per 100 km at a constant speed; Otherwise, apply a large enough value to  $f_1(x_j)$ ,  $f_2(x_j)$  and  $f_3(x_j)$ .

306 (4) Calculation of fitness values of candidate solutions. Judge relative advantages and disadvantages of candidate solutions via a specific method. The method applied in the simulation experiments of this paper: First implement non-dominated sorting of  $P_G$ , and then calculate the crowding distance of candidate solutions.

309 (5) Genetic operation to generate new candidate solutions. Select  $[0.5N]$  from  $P_G$  with the two-match method, and then carry out SBX and polynomial variation to generate new population  $Q_G$ .

311 (6) Simulation software calling to calculate the objective function value of descendant candidate solutions. Let  $\forall x_j \in Q_G$ , call *MATLAB/Simulink* software to test the performance of vehicle model corresponding to  $x_j$ . Simulate the driving status of the vehicle under the specified road conditions and obtain function values of each objective according to the returned results if performance constraint conditions can be met. To be specific,  $f_1(x_j)$  is stability factor,  $f_2(x_j)$  is the acceleration RMS value of vertical vibration at driver's seat,  $f_3(x_j)$  is the power consumption per 100 km at a constant speed; Otherwise, apply a big enough value to  $f_1(x_j)$ ,  $f_2(x_j)$  and  $f_3(x_j)$ .

317 (7) Evaluation population updating. Obtain new evaluation population with specific strategies. The method applied in the simulation experiments of this paper: First, let  $R_G = Q_G \cup$ , implement non-dominated ranking of  $P_G$  and calculate the crowding distance of candidate solutions; then, select  $N$  candidate solutions from  $R_G$  based on the ranking results to generate new population  $P_{G+1}$ ; finally, circulate through  $G = G + 1$ .

321 (8) Output Pareto optimum solution set  $P_{G+1}$  and finish evaluation if the end conditions can be met;

322 Otherwise, turn to Step (5).  
323 In Step (3) and Step (6), assign a value large enough to  $f_1(x_j)$ ,  $f_2(x_j)$  and  $f_3(x_j)$ , respectively, which means  
324 that due to its unsuitable handling stability, poor ride comfort and economy, this solution is not directly eliminated  
325 for storing diverse genes for subsequent evolutions.

326

## 327 **6 Simulation Verification and Relate Analysis**

### 328 **6.1 Experiment Related Settings**

329 *MATLAB/M – File* was used to program realization for EV-MOEA, with the scale of evaluation population  
330 as 32, maximum generation as 100, mutation probability as 0.1 and crossover probability as 0.9. The basic  
331 parameter configuration of simulated the whole vehicle is shown in Table 3.

332 Table 3 Basic Parameters of the Vehicle

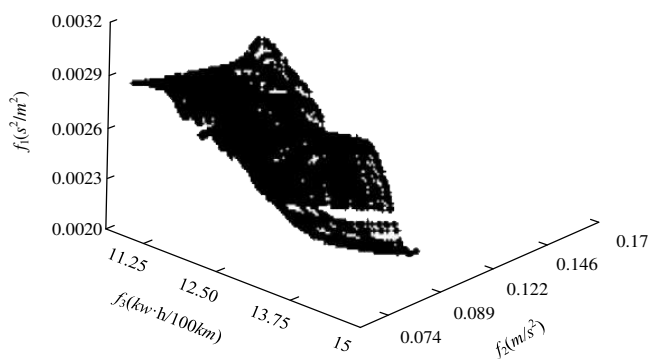
Item	Parameter	Value
	Maxmum power/kW	75
Drive the Motor	Maximum output torque/(N · m)	275
	Maxmum speed/(r · min <sup>-1</sup> )	10 000
Accumulator	Type	
	Qty./pcs	25
	Single module index	12V, 25A · h
	Total weight of vehicle (kg)	1350
Parameters of the Vehicle	Windward area (m <sup>2</sup> )	1.9
	Air resistance coefficient	0.335

### 333 **6.2 Optimization Results and Analysis**

334 The distribution of the final Pareto optimum solutions after making statistics on the results of 10 operations

335 and combining all solutions is shown in Figure 4, as well as the data of design variables. Let the working  
 336 efficiency of motor be  $E_{MC}$  and the efficiency of drive system be  $E_G$ . The statistical results of the stability factor  
 337  $f_1$  corresponding to the final Pareto optimum solutions, the root mean square value of vertical vibration  
 338 acceleration at driver's seat, the power consumption per 100 km at a constant speed and system performance are  
 339 shown in Table 5. The data in Group 0 in Table 4 and Table 5 are default settings and performance indexes of the  
 340 selected vehicle.

341



342

343 Figure 4 Distribution of Pareto Optimum Solutions after Combining the Results of 10 Operations

344

345

346 Table 4 Specific Parameters of Optimum Solutions after Combining the Results of 10 Operations

No.	$K_f / (N/m)$	$C_f / (N \cdot S/m)$	$K_r / (N/m)$	$C_r / (N \cdot S/m)$	$f_d$ (mm)	$P_e$ (kw)	$R_s$	$N_b$	$R_m$	$H_{soc}$	$L_{soc}$	$v_e$ (km/h)
0	26460	5063	37183	2532	50	41.017	1.01	25	1.00	0.71	0.60	30.00
1	24819	5129	29015	2624	55	68.916	0.61	25	0.75	0.68	0.54	31.02
2	24905	5207	29643	2601	53	69.703	0.61	25	0.74	0.71	0.46	31.21
3	25134	5473	28349	2718	47	41.569	0.65	20	1.16	0.56	0.38	32.70
4	25685	5318	28710	2794	43	36.213	0.61	20	1.08	0.68	0.41	32.64
5	24986	5067	27965	2591	51	35.951	0.60	20	1.12	0.67	0.41	30.69
6	27359	6137	29047	2548	49	69.218	0.61	25	0.75	0.81	0.45	30.95
7	26741	6243	27934	2501	45	69.026	0.61	25	0.76	0.81	0.44	32.95
8	25834	6154	26075	2856	39	41.001	0.67	20	1.18	0.56	0.40	32.74
9	24378	5409	28437	2673	41	68.667	0.59	25	0.75	0.80	0.45	30.93
10	24953	5173	25712	2613	57	36.759	0.62	20	1.23	0.68	0.42	32.52

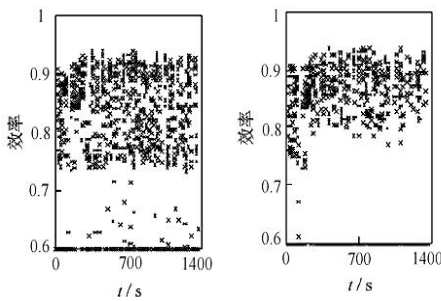
Table 5 System Performance Corresponding to Pareto Optimum Solutions after Combining the Results of 10 Operations

No.	Objective Function Value			System Performance	
	$f_1/(s^2/m^2)$	$f_2/(m/s^2)$	$f_3(kw \cdot h/100km)$	$E_{MC}$	$E_G$
0	0.0023	0.114	15.89	0.79	0.89
1	0.0026	0.101	13.73	0.91	0.91
2	0.0027	0.112	13.95	0.89	0.93
3	0.0029	0.109	13.96	0.75	0.94
4	0.0025	0.112	14.25	0.86	0.93
5	0.0023	0.111	14.37	0.85	0.92
6	0.0021	0.110	13.98	0.89	0.91
7	0.0029	0.109	13.29	0.71	0.92
8	0.0023	0.106	13.17	0.88	0.94
9	0.0024	0.108	14.56	0.85	0.93
10	0.0025	0.104	14.59	0.79	0.91

348 It can be found from the data in Table 5 that the optimized system has reduced the acceleration RMS value of  
 349 vertical vibration at driver's seat and the power consumption per 100 km at a constant speed under the premise of  
 350 guaranteeing vehicle handling stability. In the optimized system, stability factors have increased by 9.5%, the  
 351 acceleration RMS value of vertical vibration at driver's seat has decreased by 5.1% and the power consumption  
 352 per 100 km at a constant speed has decreased by 8.8% on average, respectively.

353 As for the efficiency of the system, the efficiency of motor and driving system has increased by 6.1% and 3.8%  
 354 on average, respectively, which implies that the working efficiency of major components of the vehicle has  
 355 increased after optimization and each subsystem has better matched, so the multi-performance optimization  
 356 proposed in this paper can improve the total working efficiency of BEVs.

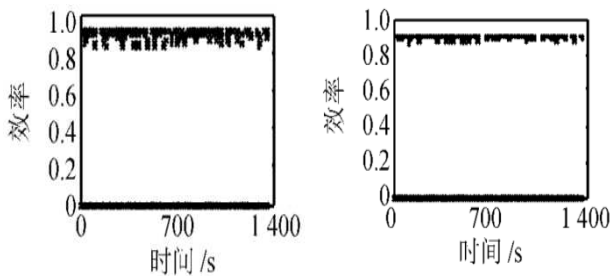
357 As an example, the optimization solution of Group 1 was compared with the system before optimization.  
 358 Figure 5 and Figure 6 show the comparison results of the efficiency of motor and driving system, respectively.



359  
360 (a) Before optimization (b) After optimization

361 Figure 5 Comparison Figure on Working Efficiency of Motor

362 According to Figure 5, the efficiency of motor was mainly within [0.7, 0.95] before optimization but within  
363 [0.8, 0.95] after optimization, while the working points of optimized motor were highly distributed in the high  
364 efficient areas after comparing the distribution diagram on working points of motor, which indicates that the  
365 efficiency of optimized motor has been significantly improved, which is further helpful to improve the economy  
366 of BEVs.



367  
368 (a) Before optimization (b) After optimization

369  
370 Figure 6 Efficiency Comparison of Driving System

371  
372 According to Figure 6, the efficiency of driving system was within [0.8, 0.9] approximately before  
373 optimization but mainly within [0.85, 0.95] after optimization, which shows that the efficiency of driving system  
374 after optimization is superior to that before optimization, which is helpful to improve the comprehensive  
375 efficiency of BEVs.

376    **7 Conclusions**

377       To address the multi-performance optimization of BEVs, this paper proposed the corresponding model and  
378       algorithm for the multi-objective evaluation based on Pareto optimum principle with handling stability, ride  
379       comfort and economy as optimization objectives and improved ride comfort and economy under the premise of  
380       guaranteeing vehicle handling stability. The effectiveness of the method has been verified through simulation test  
381       and the following conclusions have been made.

382       (1) Multi-objective optimization algorithm of BEVs proposed based on Pareto optimum principle can  
383       improve ride comfort of vehicles and reduce energy consumption of batteries under the premise of guaranteeing  
384       handling stability. According to the simulation experiment, the algorithm has optimized multi-performance target  
385       collaboratively such as the safety, comfort and energy conservation of BEVs.

386       (2) The working efficiency of motor and driving system of BEVs have been improved differently after  
387       optimization, which means that each subsystem has been better matched after optimization and BEVs show a  
388       better performance.

389       (3) The method proposed in this paper makes it unnecessary to simplify the multi optimization objectives  
390       into one, which avoids the adverse influence caused by the weighted sum of different objectives, providing many  
391       groups of optimum solutions.

392

393    **Availability of data and materials**

394       All data generated or analysed during this study are included in this published article [and its supplementary  
395       information files].

396    **Acknowledgments**

397       We hereby would like to extend our gratitude towards the sponsors that supported this study, the National

398 Key Research and Development Plan (Grant No.: 2016YFB0100900).

399 **Authors' Contributions**

400 Yawei Chen and Qian Cheng wrote the manuscript; Jurui Liu was in charge of the whole trial, review and  
401 edition; Xixiang Hao and Chenheng Yuan assisted with review. All authors read and approved the final  
402 manuscript.

403 **Authors' Information**

404 Yawei Chen was born in Dingxi, Gansu, China, in 1993. He received the M.S. in Vehicle engineering in 2019  
405 from Chongqing Jiaotong University. He is currently a vehicle Engineer at the China Automotive Engineering  
406 Research Institute. His current research interests include electric vehicle and dynamics.

407 Qian Cheng was born in Chongqing, China, in 1993. He received the B.S. degree in automobile support  
408 engineering in 2016, the M.S. degree in vehicle operation engineering in 2019 from Chongqing Jiaotong  
409 University. He is currently a vehicle Engineer at the China Automotive Engineering Research Institute. His current  
410 research interests include electric vehicle and dynamics.

411 Jurui Liu was born in Changchun, Jilin, China, in 1988. She received the M.S. in HVAC engineering from  
412 the Jilin Jianzhu University, Jilin, China, in 2019. She currently works in Beijing Yunshan World Information  
413 Technology company. Her current work includes automatic control, big data and machine learning.

414 Xixiang Hao was born in Anqing, Anhui, China, in 1991. He received the M.S. in Traffic and transportation  
415 from Chongqing Jiaotong University, Chongqing, China, in 2019. He currently works in Zhejiang Sanhua  
416 Automotive components Co. LTD. His current research interests include Intelligent control and Thermal  
417 management of equipment.

418 Chenheng Yuan was born in Xichong, Sichuan, China, in 1984. He received the Ph.D. degrees in power  
419 machinery and engineering from the Beijing Institute of Technology, Beijing, China, in 2015. From 2016 to 2019,  
420 He was an Associate Professor with Automobile Application Engineering Department, Chongqing Jiaotong

421 University. Since 2019, he has been a Professor with the School of Traffic and Transportation, Chongqing  
422 Jiaotong University. His current research interests include electric vehicle, hybrid electric system and electronic  
423 control.

424 **Funding**

425 Supposed by the National Key Research and Development Plan (Grant No.: 2016YFB0100900).

426 **Competing Interests**

427 The authors declare no competing financial interests.

428 **Author Detail**

429 <sup>1</sup>China Automotive Engineering Research Institute Co., Ltd. , Chongqing 401147, China. <sup>2</sup>Beijing Yunshan  
430 World Information Technology Co., Ltd., Beijing 100006, China. <sup>3</sup>Zhejiang Sanhua Auto Parts Co., Ltd.,  
431 Hangzhou, Zhejiang 311200, China. <sup>4</sup>Chongqing Jiaotong University College of Traffic & Transportation,  
432 Chongqing 400074, China.

433 **References**

- 434 [1] ELS P S, UYS P E. Investigation of the applicability of the dynamic-Q optimization algorithm to vehicle suspension design[J].  
435 Mathematical & Computer Modeling, 2003, 37( 9/10) :1029-1046.  
436 [2] GONCALVES J P C, AMBRSSIO J A C. Optimization of vehicle suspension systems for improved comfort of road vehicles  
437 using flexible multi-body dynamics [J]. Nonlinear Dynamics, 2003, 34( 1) : 113-131.  
438 [3] YANG Y, REN W, CHEN L, et al. Study on ride comfort of tractor with tandem suspension based on multi-body system  
439 dynamics [J]. Applied Mathematical Modelling, 2009, 33(1) : 11-33.  
440 [4] YANG Rongshan, YUAN Zhongrong, HUANG Xiangdong, et al. Research on the Collaborative Optimization of Vehicle  
441 Handling Stability and Ride Comfort [J]. Automotive Engineering, 2009, 31 (11): 1053-1059.  
442 [5] XU Haijiao. Analysis of Vehicle Handling Stability and its Multi-objective Optimization Design [D]. Handan: Hebei University  
443 of Engineering, 2015, 51-62.

- 444 [6] SONG Kang, CHEN Xiaokai, LIN Yi. Multi-objective Optimization of Vehicle Driving Dynamics Performance [J]. Journal of  
445 Jilin University (engineering science edition) 2015, 45 (2): 352-357.
- 446 [7] CHEN Yikai, HE Jie, ZHANG Weihua et al. Improvement of Ceiling Control Strategy for the Suspension System of Multi-axle  
447 Heavy Truck [J]. Journal of Agricultural Machinery, 2011, 42 (6): 16-22.
- 448 [8] ZHENG Zhifei, LIU Jianli, XU Zhongming, YANG Jianguo et al. Optimization of Commercial Vehicle Suspension Parameters  
449 for Smoothness and Road Friendliness [J]. Automotive Engineering, 2014, 36 (7): 889-893.
- 450 [9] YANG Kun. Simulation and Multi-objective Optimization of Smoothness and Road Friendliness of Six-axle Semi-trailer Train  
451 [D]. Changchun: Jilin University, 2017, 58-75.
- 452 [10] ZHOU Feikun. Research on Dynamic System Parameter Matching and Vehicle Control Strategy of Battery Electric Vehicles  
453 [D]. Changchun: Jilin University, 2013.
- 454 [11] ZHANG Kangkang. Research on the Efficiency Optimization Method of Battery Electric Vehicles [D]. Beijing: Tsinghua  
455 University, 2014.
- 456 [12] LIN Jiahao, ZHANG Yahui. Virtual Excitation Method for Random Vibration [M]. Beijing: Science Press, 2004:42-57.
- 457 [13] YU Zhisheng. Automobile Theory [M]. Beijing: Machinery Industry Press, 2009.
- 458 [14] ZHANG Jingmei. Research on Dynamic Performance and Multi-objective Optimization of Heavy-duty Vehicles [D]. Beijing:  
459 Beijing Jiaotong University, 2018.
- 460 [15] YGANG Guansi, LI Shaobo, QU Jinglei et al. Multi-objective Optimization of Hybrid Vehicle Based on Pareto Optimal  
461 Principle [J]. Journal of Shanghai Jiaotong University, 2012, 46 (8): 1297-1309.